PHYSICAL REVIEW B VOLUME 33, NUMBER 5 1 MARCH 1986

Magnetic properties of Al-Si-Mn and Al-Mn quasicrystals and amorphous films

J. J. Hauser, H. S. Chen, and J. V. Waszczak
AT&T Bell Laboratories, Murray Hill, New Jersey 07974
(Received 18 September 1985)

Unlike the orthorhombic phase, the icosahedral phase of $Al_{86}Mn_{14}$ exhibits a local magnetic moment. The effective moment of icosahedral-phase Al-Mn and Al-Si-Mn alloys increases with Mn concentration up to a maximum of $(1.5 \pm 0.5)\mu_B$. The amorphous and icosahedral phases of Al-Si-Mn have similar magnetic properties for Si concentrations $\lesssim 6$ at.%, and the moments seem to order in a spin-glass state. For Si concentrations $\gtrsim 30$ at.%, amorphous Al-Si-Mn orders ferromagnetically.

Shechtman, Blech, Gratias, and Cahn[1] have observed long-range icosahedral orientational order in rapidly quenched $Al_{86}Mn_{14}$. More recently,[2] superlattice structures with icosahedral point-group symmetry (so-called quasicrystals) have been observed in melt-quenched $Al_{74}Si_6Mn_{20}$ and $Al_{72}Si_6Mn_{22}$ alloys. Mathematical models[3–5] based on three-dimensional Penrose tilings can accurately reproduce the diffraction patterns from these quasicrystals and also predict two types of Mn sites for them. The results of a recent Mössbauer study[6] are consistent with two sites, but a still more recent Mössbauer study[7] obtained data more consistent with a distribution of Mn sites. Also, a recent NMR study[8] indicates that the quadrupolar structure of the ^{55}Mn resonance which one would expect based on two Mn sites is absent. Both Refs. 7 and 8 conclude that there is no significant difference between the relative broad electric-field-gradient (EFG) distributions at the Mn sites in icosahedral (I) and amorphous (a) $Al_{86}Mn_{14}$, and Ref. 8 further establishes that the EFG distributions for both Al and Mn sites are broader in I-$Al_{72}Si_6Mn_{22}$ than in either I- or a-$Al_{86}Mn_{14}$. Such structural differences could give rise to different magnetic properties; hence we report here a magnetic study of Al-Mn and Al-Si-Mn alloys in both icosahedral and amorphous forms.

The quasicrystal samples were prepared from alloys melted inductively in a boron-nitride crucible under an argon atmosphere and subsequently made into ribbons approximately 1 mm wide and 30 μm thick by the melt-spinning technique. The amorphous films were sputtered from the corresponding induction-melted alloy onto a sapphire substrate. The film was then scraped from the substrate with a sapphire slide to avoid magnetic contamination. The resulting flakes were measured in a low-field (4 Oe) ac susceptibility apparatus at 10 kHz and in a high-field (12.8 kOe) susceptibility apparatus with the Faraday method. The magnetization was obtained by integrating the ac-susceptibility versus magnetic field curve. The structure of the samples was determined by transmission electron microscopy (TEM), electron diffraction, and by x-ray diffraction. The TEM and electron-diffraction studies were performed either on thinned-down 30-μm-thick ribbons or on free-standing films, or directly on 1500 Å free-standing films obtained by deposition on a NaCl substrate which was subsequently dissolved.

Before discussing their magnetic properties, we will make a few remarks on the structure of these alloys. While melt-spun $Al_{86}Mn_{14}$ *ribbons* are icosahedral for 6-at.% Si or less and amorphous for $\geqslant$20-at.% Si, $Al_{86}Mn_{14}$ *films* are always amorphous even for deposition temperatures as high as 780 K. This is surprising since the icosahedral phase of $Al_{86}Mn_{14}$ ribbons quickly transforms[1,2] ($\simeq 10$ min) into a stable Al_6Mn orthorhombic (O) phase when heated at 680 K. Furthermore, film deposition at 880 K yields O-Al_6Mn and consequently, the icosahedral structure is never observed in films. The greater stability of a-$Al_{86}Mn_{14}$ films is not due to argon inclusions since the films deposited at high temperatures are essentially argon free.

The major results of the present study are shown in Fig. 1. (The O-$Al_{86}Mn_{14}$ was obtained by heating the I-$Al_{86}Mn_{14}$ ribbon for 10 min at 780 K under an argon atmosphere.) Figure 1 shows that the susceptibility (χ) of O-$Al_{86}Mn_{14}$ is temperature independent and therefore that O-$Al_{86}Mn_{14}$ does not exhibit a local moment. On the other hand, the susceptibility of I-$Al_{86}Mn_{14}$ displays a pronounced temperature dependence which implies the presence of a local magnetic moment. This temperature dependence increases with increasing Mn content, as shown by the curves for 18- and 20-at.% Mn and the χ_{ac} curve for $Al_{80}Mn_{20}$ quite similar to that measured for $Al_{72}Si_6Mn_{22}$. Consequently, all the binary and ternary icosahedral alloys with Mn concentrations $\geqslant 14$ at.% are magnetic, and a Curie-Weiss fit of the susceptibility between 10 and 300 K yields an average antiferromagnetic interaction and the magnetic moments p_{eff} listed in Table I, which shows that p_{eff} increases with increasing Mn content in both the binary and ternary alloys. One should, however, be careful not to confuse the values of p_{eff} obtained in the high-field measurement with those obtained in the low-field ac measurement: The latter were fitted to a Curie-Weiss law between 10 and 40 K and, as shown in Table I, are systematically higher. Furthermore, there are deviations from the Curie-Weiss law below 10 K (χ is lower than the Curie-Weiss value) which suggests the presence of a magnetic transition. Indeed, a low-field (4 Oe) ac-susceptibility measurement of I-$Al_{80}Mn_{20}$ (upper curve with solid dots and inset curve in Fig. 1) reveals a susceptibility peak not seen in the high-field (12.8 kOe) dc-susceptibility measurement. However, the difference between χ_{dc} and χ_{ac} for I-$Al_{80}Mn_{20}$ may arise not only from the differences in applied fields but also because the ac susceptibility was measured on half the mass used in the dc-susceptibility measurement.

Figure 2 shows the ac susceptibility for I-$Al_{72}Si_6Mn_{22}$, and compares it to the susceptibilities of an amorphous film of the same composition and an icosahedral ribbon with lower Mn content. The susceptibility of a-$Al_{72}Si_6Mn_{22}$ is similar to the susceptibilities of both I-$Al_{72}Si_6Mn_{22}$ and I-

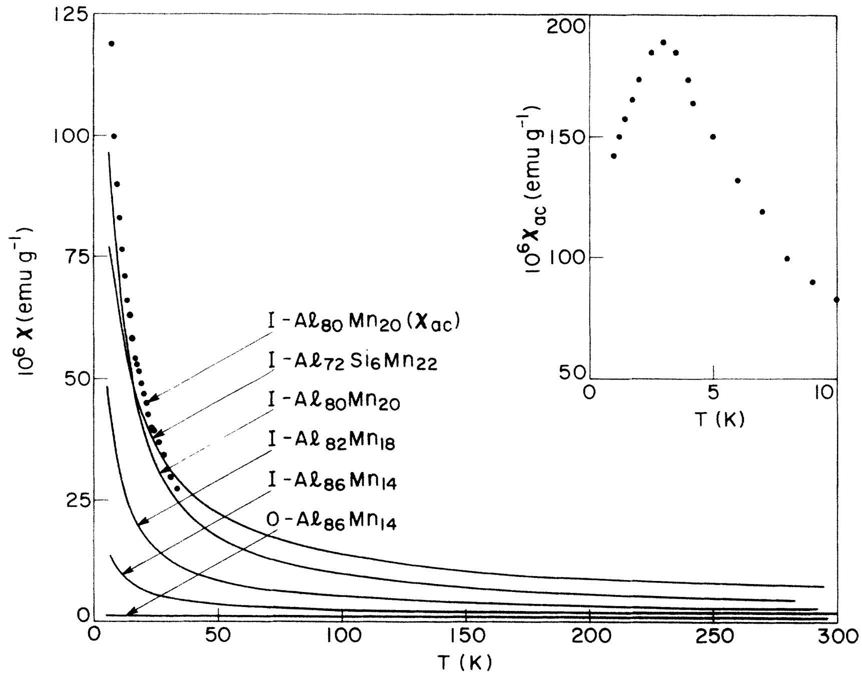

FIG. 1. The curves refer to the temperature dependence of the high-field (12.8 kOe) dc susceptibility for icosahedral (I) quasicrystals and the orthorhombic (O) crystal; the solid dots represent the low-field (4 Oe) ac susceptibility for I-$Al_{80}Mn_{20}$ which is extended in the inset for $T \leq 10$ K.

$Al_{78}Si_6Mn_{16}$ (the small increase in χ below 2.5 K for a-$Al_{72}Si_6Mn_{22}$ may arise from a small amount of intrinsic or extrinsic ferromagnetism). The susceptibilities of a-$Al_{86}Mn_{14}$ and a-$Al_{85}Mn_{15}$ are also similar to that shown in Fig. 1 for I-$Al_{86}Mn_{14}$. Furthermore, the application of increasing dc magnetic fields leads to the progressive elimination of the susceptibility peak of a-$Al_{72}Si_6Mn_{22}$ (Fig. 2) and the same effect has been observed for icosahedral ribbons. This suggests that the susceptibility peak arises from a spin-glass interaction with spin freezing at a temperature (T_{SG}) corresponding to the maximum in χ. As summarized in Table I, this spin-glass interaction has been observed for icosahedral ribbons and amorphous films with Si concentrations ≤ 6 at.% and 16 at.% $\leq$ Mn concentration ≤ 22 at.%. The similarity between the magnetic properties of icosahedral and amorphous phases for Si concentrations ≤ 6 at.% (Fig. 2) agrees with the similarity observed between these phases in Mössbauer[7] and NMR[8] studies.

We shall now study the increase of p_{eff} with increasing Mn content in greater detail. Figure 3 displays the concentration dependence of p_{eff} as obtained from a Curie-Weiss fit of the high-field susceptibility between 10 and 300 K (the

TABLE I. Magnetic properties of Al-Mn and Al-Si-Mn alloys (Si ≤ 6 at.%).

Sample	Type	Structure	T_{SG} (K)	T_c (K)	$-\theta$ (K)	p_{eff} (μ_B)	$10^6\chi_{4.2\,K}$ (emu g^{-1})
$Al_{86}Mn_{14}$[a]	Ribbon	Orthorhombic	...	...	...	0	1.5
$Al_{86}Mn_{14}$[a]	Ribbon	Icosahedral	...	...	8.7	0.5	17.5
$Al_{84}Mn_{16}$[a]	Ribbon	Icosahedral	...	...	5	0.62	32.2
$Al_{84}Mn_{16}$	Ribbon	Icosahedral	< 1.0	...	4	0.75	51.5
$Al_{82}Mn_{18}$[a]	Ribbon	Icosahedral	...	...	5	0.75	47.9
$Al_{82}Mn_{18}$	Ribbon	Icosahedral	1.5	...	4	0.97	79.4
$Al_{80}Mn_{20}$[a]	Ribbon	Icosahedral	...	...	4	1.06	96.4
$Al_{80}Mn_{20}$	Ribbon	Icosahedral	3	...	1	1.12	164
$Al_{78}Si_6Mn_{16}$	Ribbon	Icosahedral	2.5	...	4.5	1.00	77
$Al_{77}Si_3Mn_{20}$	Ribbon	Icosahedral	3.5	...	3.0	1.28	168
$Al_{72}Si_6Mn_{22}$[a]	Ribbon	Icosahedral	...	...	10	1.17	77
$Al_{72}Si_6Mn_{22}$	Ribbon	Icosahedral	3.5	...	11	1.55	115
$Al_{72}Si_6Mn_{22}$	Film	Amorphous	6	...	2.3	1.41	150

[a]High-field (12.8 kOe) dc susceptibility while all others are low-field (4 Oe) ac-susceptibility measurements.

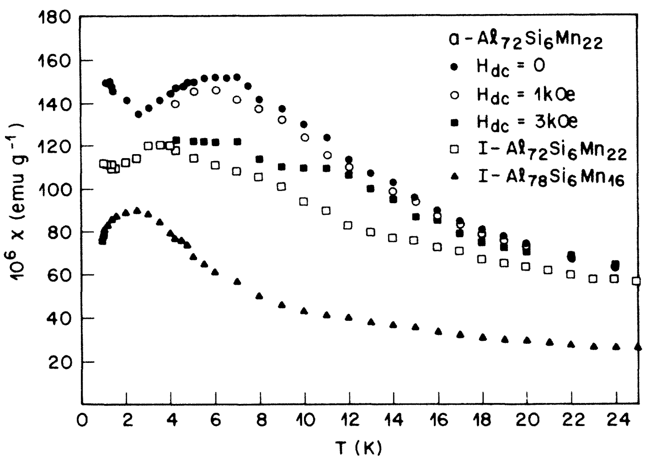

FIG. 2. Temperature dependence of the ac susceptibility for icosahedral ribbons and an amorphous film.

same data are listed in Table I). The monotonic increase in p_{eff} with Mn content shown in Fig. 3 leads to two important conclusions: that the small moment seen in I-$Al_{86}Mn_{14}$ is an intrinsic property of the icosahedral phase and, since p_{eff} for I-$Al_{72}Si_6Mn_{22}$ is in excellent agreement with the p_{eff} values for the binary alloys that the Mn atoms occupy very similar positions in the binary and ternary icosahedral phases. Furthermore, Fig. 3 shows that $p_{\mathrm{eff}} \propto C_{\mathrm{Mn}}^2$ within experimental error. This result agrees with the fact that the small amount of equilibrium-dissolved Mn (up to 0.32 at.%) in Al has a nonmagnetic localized d state.[9,10] The quadratic dependence on C_{Mn} suggests that the local moment in the icosahedral phase arises from a pair interaction between the Mn localized d wave functions. It is also interesting that the maximum $p_{\mathrm{eff}} \simeq 1.2\mu_B$ occurs at about 20-at.% Mn which has been suggested[4] as the optimum icosahedral concentration.

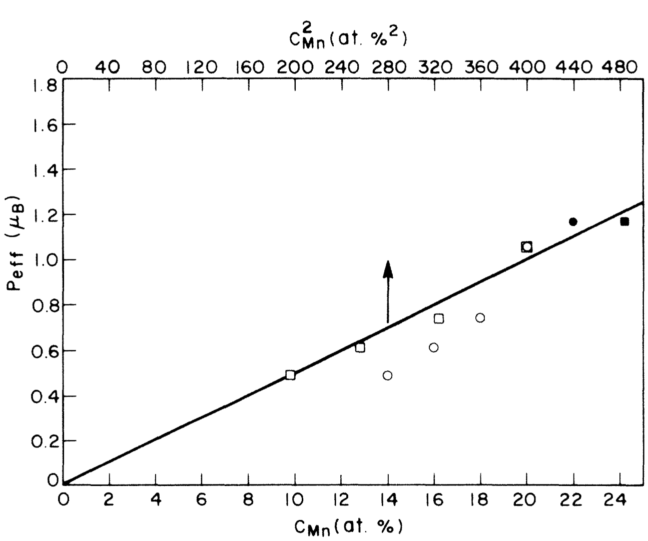

FIG. 3. Effective moment p_{eff} as a function of Mn concentration (dots) and as a function of the square of the Mn concentration (squares); the open symbols refer to binary Al-Mn alloys and the solid symbols to the Al-6-at.% Si-Mn alloy.

There are, however, obvious problems with the fit presented in Fig. 3. First, one knows that the icosahedral phase cannot exist down to $C_{\mathrm{Mn}} \simeq 0$ and consequently, that our conclusion of no moment at low C_{Mn} applies only to a stabilized icosahedral phase with low C_{Mn}. Furthermore, a few at.% of free Al are always observed with x-ray diffraction and NMR[8] in the binary alloys with low Mn content, and a few at.% of secondary T phase is present[2] in the $Al_{80}Mn_{20}$ alloy. It is therefore possible that if one considered only the Mn present in the icosahedral phase that p_{eff} would have a less-pronounced dependence on C_{Mn} than that shown in Fig. 3. However, even if the exact amount of free Al were known one could not correct the data shown in Fig. 3 by assuming that all the Mn is present only in the icosahedral phase. Indeed, although the amount of equilibrium-dissolved Mn is small, rapidly quenched melts can dissolve[11] up to 4.7-at.% Mn (and melt-spun ribbons even more) and such metastable alloys could be weakly magnetic. Despite these limitations, the quadratic fit shown in Fig. 3 is most probably correct since the ternary alloy is known[2] to be single phased and its p_{eff} value is in excellent agreement with those of the binary alloys.

We now examine the magnetic properties of amorphous ribbons and films with high Si content. As shown in Fig. 4 by both susceptibility and magnetization curves, an a-$Al_{26}Si_{40}Mn_{24}$ ribbon displays a ferromagnetic transition between 100 and 110 K. Figure 4 also shows that this transition is unaffected by the quenching rate: Two ribbons quenched at different rates have the same Curie temperature (T_c) of 110 K as determined by susceptibility measurements. On the other hand, an amorphous film of the same composition displays a completely different behavior: The susceptibility data shown in Fig. 4 can be fitted between 10 and 160 K by a Curie-Weiss law with the parameters listed in Table II. There is, however, a pronounced deviation from the Curie-Weiss law below 10 K which, when coupled with magnetization measurements indicates a weak ferromagnetic transition at $T_c \simeq 6$ K. Consequently, in contrast to the alloys with low Si content, where icosahedral ribbons and amorphous films had similar magnetic properties, amorphous films, and amorphous ribbons with high Si content have different magnetic properties.

An attempt to understand the origin of the ferromagne-

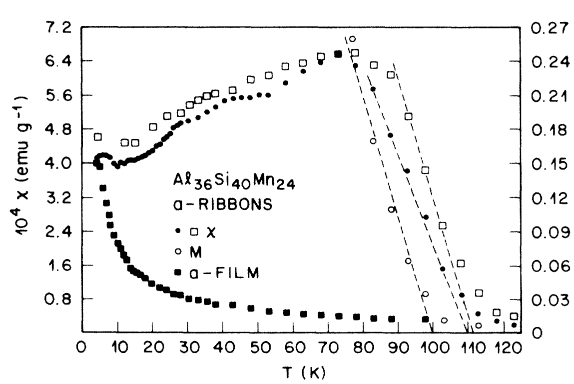

FIG. 4. Temperature dependence of the ac susceptibility and magnetization for amorphous (a) ribbons and an a-film. The solid and open dots pertain to the same ribbon while the open squares refer to another ribbon obtained by faster quenching.

TABLE II. Magnetic properties of Al-Si-Mn alloys (Si $\geq$ 20 at.%).

Sample	Type	Structure	T_c (K)	$-\theta$ (K)	p_{eff} (μ_B)	$10^6\chi_{4.2\ \mathrm{K}}$ (emu g^{-1})
$Al_{25}Si_{50}Mn_{25}$	Ribbon	Amorphous	12	41	1.27	82
$Al_{34}Si_{40}Mn_{26}$	Ribbon	Amorphous	43	38	1.53	94
$Al_{36}Si_{40}Mn_{24}$	Ribbon	Amorphous	105	−44	1.83	412
$Al_{36}Si_{40}Mn_{24}$[a]	Ribbon	Amorphous	105	77	1.42	460
$Al_{36}Si_{40}Mn_{24}$	Film	Amorphous	6	10	1.96	400
$Al_{38}Si_{40}Mn_{22}$	Ribbon	Amorphous	105	...	...	154
$Al_{40}Si_{40}Mn_{20}$	Ribbon	Amorphous	105	...	...	157
$Al_{46}Si_{40}Mn_{14}$[b]	Ribbon	Amorphous	...	...	...	155
$Al_{50}Si_{30}Mn_{20}$	Ribbon	Amorphous	120	54	1.73	354
$Al_{56}Si_{30}Mn_{14}$	Ribbon	Amorphous	...	−30	2.23	38
$Al_{66}Si_{20}Mn_{14}$[b]	Ribbon	Amorphous	...	...	...	8

[a]Ribbon was quenched faster than previous one (line above).
[b]χ is essentially temperature independent.

tism observed in the a-$Al_{36}Si_{40}Mn_{24}$ ribbon by varying the Si and Mn content (summarized in Table II) failed to yield any clue. Indeed, the various parameters listed in Table II do not exhibit any specific trend and there is appreciable scatter in the values of θ (see $Al_{36}Si_{40}Mn_{24}$ and $Al_{56}Si_{30}Mn_{14}$ in Table II). A possible source for the ferromagnetism of $Al_{36}Si_{40}Mn_{24}$ might be that its composition closely resembles that of a Heusler alloy[12] of the Cu_2MnAl type. However, as shown in Table II, the corresponding alloy ($Al_{25}Si_{50}Mn_{25}$) is only weakly ferromagnetic, ruling out such an explanation. The only conclusion one can draw from Table II is that amorphous ribbons with 30–40-at.% Si are ferromagnetic for Mn concentrations between 20 and 26 at.%. It is also worth pointing out that, except for the sample with 30-at.% Si, magnetism disappears for a Mn concentration of 14 at.% (Table II), similar to the behavior of the low Si concentration ($\leq$ 6 at.%) samples.

In conclusion, while O-$Al_{86}Mn_{14}$ does not exhibit a local magnetic moment, the quasicrystalline icosahedral phase does, and this moment increases with increasing Mn content. For Si concentrations $\leq$ 6 at.% the magnetic properties of amorphous films and icosahedral ribbons are similar. These moments seem to order in a spin-glass state for Si concentrations $\leq$ 6 at.% and into a ferromagnetic state for Si concentrations $\geq$ 30 at.%. The ferromagnetism is much weaker in amorphous films than in amorphous ribbons.

We would like to thank R. J. Felder for his technical assistance and J. M. Gibson for performing the electron-diffraction experiments.

[1]D. Shechtman, I. Blech, D. Gratias, and J. W. Cahn, Phys. Rev. Lett. **53**, 1951 (1984).
[2]C. H. Chen and H. S. Chen (unpublished).
[3]D. Levine and D. J. Steinhardt, Phys. Rev. Lett. **53**, 2477 (1984).
[4]V. Elser, Phys. Rev. B (to be published).
[5]M. Duneau and A. Katz (unpublished).
[6]L. J. Swartzendruber, D. Shechtman, L. Bendersky, and J. W. Cahn, Phys. Rev. B **32**, 1383 (1985).
[7]M. Eibschutz, H. S. Chen, and J. J. Hauser, Phys. Rev. Lett. **56**, 169 (1986).
[8]W. W. Warren, H. S. Chen, and J. H. Hauser, Phys. Rev. B **32**, 7614 (1985).
[9]A. B. Kaiser, J. Phys. C **3**, 409 (1970).
[10]J. J. Hauser, Phys. Rev. B **5**, 1830 (1972).
[11]M. Hansen, *Constitution of Binary Alloys* (McGraw-Hill, New York, 1958), p. 113.
[12]C. C. M. Campbell, J. Phys. F **5**, 1931 (1975).